SMAR 2015 – Third Conference on Smart Monitoring,
Assessment and Rehabilitation of Civil Structures

SMAR 2015

Repairing cracks in concrete beams using cold-drawn SMA short fibers

Eunsoo Choi[1], DongJoo Kim[2], Young-Soo Chung[3], Joowoo Kim[4],
Chanyeong Jeon[1], and Kyoung-Teak Yang[5]

[1]Hongik university, Seoul, Korea/ [2]Sejong University, Seoul, Korea/
[3]Chung-Ang University, Seoul, Korea/ [4]Semyung University, Jechun, Korea
[5]Daelim Colleage, Kyounggi, Korea

ABSTRACT: In this study, crack-closing tests of mortar beams reinforced by shape memory alloy (SMA) short fibers were performed. After this, crack-repairing tests were also conduted. For this purpose, NiTi SMA fibers with a diameter of 0.965 mm and a length of 30 mm were made from SMA wires of 1.0 mm diameter by cold drawing. Four types of SMA fibers were prepared, namely, straight and dog-bone-shaped fiber and the two types of fibers with paper wrapping in the middle of the fibers. The paper provides an unbonded length of 15 mm. For bending tests, six types of mortar beams with the dimensions of 40 mm x 40 mm x 160 mm (BxHxL) were prepared. The SMA fibers were embedded at the bottom center of the beams along with an artificial crack of 10 mm depth and 1 mm thickness. This study investigated the influence of SMA fibers on the flexural strength of the beams from the measured force-deflection curves. After cracking, the beams were heated at the bottom by fire to activate the SMA fibers. Then, the beams recovered the deflection, and the cracks were closed. This study evaluated crack-closing capacity using the degree of crack recovery and deflection-recovery factor. For repairment, eposy was applied into the cracks before heating the SMA fibers. The repaired beams recovered their original flexural strength.

1 INTRODUCTION

Shape memory alloys (SMAs) have been used to repair cracks in concrete because they can provide the mechanical force required to close cracks using the unique properties of the shape memory effect and superelasticity. The recovery stress of SMAs induced by the shape memory effect can close open cracks. Short fibers is used to closing cracks or recover the deflection of a member using the recovery stress of SMA fibers (Li et al, 2006; Deng et al., 2006). For the repair of concrete-cracks, adhesive between cracks is required following the introduction of recovery stress on the SMA fibers (Li et al., 2007; Li et al., 2008). Recently, Choi and Kim (Choi et al., 2014; Kim et al., 2014) suggested a new concept of straight short fibers using martensitic SMAs. The shape of the fibers is straight, and their bulged end part increases bond strength. They also conducted bending tests of concrete beams reinforced by these straight SMA short fibers (Choi et al, 2015). After cracking, the SMA fibers were heated by flame to induce the shape memory effect of the SMAs, and recovery stress developed close the cracks. Based on the literature review, for crack-repairing, SMA fibers should be combined with an adhesive, such as epoxy, which bonds cracking surfaces together and recovers the tensile strength of concrete. A critical point for repairing cracks in concrete is how to inject adhesive

into cracks. In this paper, a new injecting method is proposed to repair cracks in concrete using SMA short fibers, which have been newly devised recently.

2 SMA FIBERS

2.1 NiTi and NiTiNb SMA fiber

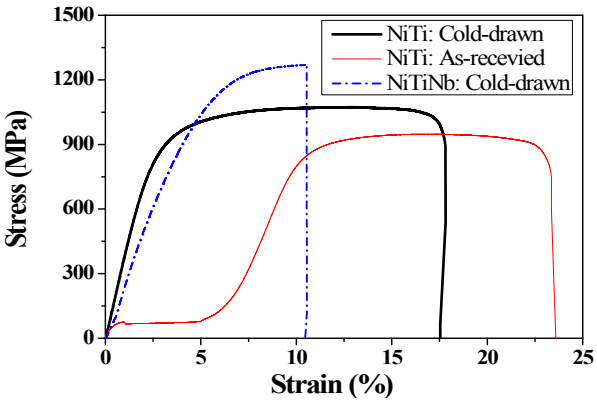

Figure 1. Comparison of tensile behavior of cold-drawn and as-received SMA wires (Choi et al., 2015)

SMA wires of $Ni_{50.47}$-$Ti_{49.53}$ (at. %) with a 1.0 mm diameter were prepared to make SMA short fibers. The diameter of the SMA wires was reduced by using the cold-drawing method to input strain on the wires. Their diameter became 0.965 mm. The tensile behavior of the cold-drawn SMA wire was reported in a previous paper as shown in Fig. 1 (Choi et al., 2015). It seems that the cold-drawing removed the elastic phases of the first elastic and transition of state. For the cold-drawn and as-received SMA wire, secant Young's moduli at 0.3% strain were estimated as 440 and 172 MPa, respectively. After the cold-drawing, the SMA wires were cut into 30 mm lengths to be incorporated in mortar beams. This study used an alloy of Ni_{50}-Ti_{41}-Nb_9 (at. %). First, SMA wires with a diameter of 1.12 mm were manufactured. Then, the wires were annealed with 850℃ for 15 minutes to eliminate all remaining strain from inside the wires. After that, the wires were cold-drawn to a diameter of 1.0 mm. The secant Young's modulus of the wire at 1.0% strain was estimated as 237.5 MPa, and the ultimate strength was 1268 MPa at 10.5% strain.

2.2 Thickness recovery and residual stress

The SMA fibers elongated by cold-drawing and prestrained 10% recovered their thickness or diameter by heating because of the shape memory effect. Bulging at both ends of an SMA fiber occurs outside the cement composite, and in this case, the shape of the fibers is dog-bone. This study measured the diameter-recovery of cold-drawn SMA fibers with a length of 50 mm at five points. During the tests, the diameters of the fibers before and after heating were measured along the length of the fibers. Original diameters of NiTi fibers are 0.9642mm and increased to 0.9788mm (2.61%) after heating. For the NiTiNb fibers, the diameters increased from 1.0890mm to 1.1114mm (2.06%). The area recovery ratio was 5.29% and 4.21% respectivley. A pre-strained martensitic SMA under a deformation constraint generates recovery stress upon heating to above the A_f temperature. The remaining stress after cooling at room temperature is called residual stress. Figure 2 shows the recovery stress of SMA fibers with temperature variation. For the NiTi fiber, the recovery stress reached 360.5 Mpa at 149.0℃. Then the stress became 28.8 Mpa at 25.7℃. For the NiTiNb fiber, the stress went up 364.3 Mpa at 228.4℃,

and it went down 229.9 Mpa at 24.9℃. The residual stress of the NiTi fibers with ambient temperarure was much smaller than the corresponding value of the NiTiNb fiber.

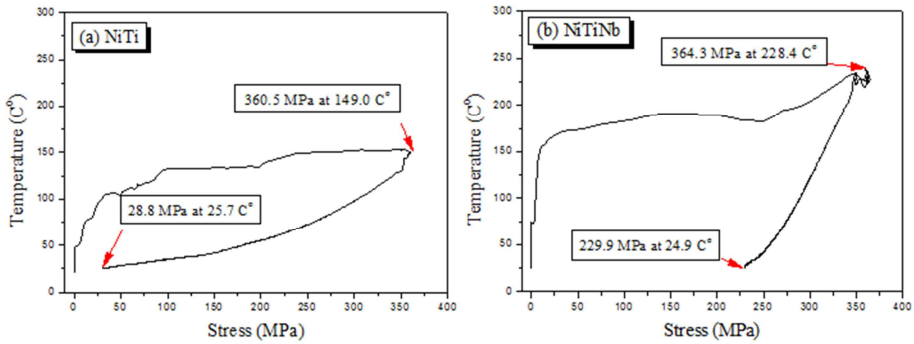

Figure 2 Recovery stress of SMA fibers with temperature variation

2.3 *Types of SMA short fibers*

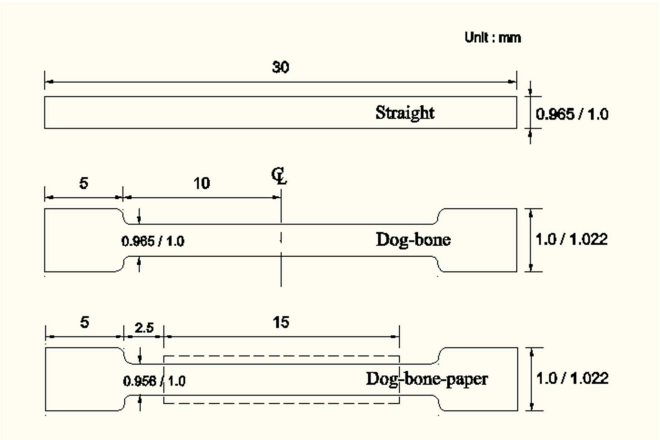

Figure 3 Types of SMA fibers

This study used three types of SMA short fibers for both alloys and their length was 30 mm. The types were straight (ST), dog-bone-shaped (DG), and dog-bone-shaped with paper wrapping (DGP) in the middle. The dog-bone-shaped fibers were manufactured by heating only a 5 mm length at each end. The paper wrapping with a length of 15 mm in the middle increased the unbonded length of a fiber. Schematic drawing of SMA fibers are shown in Fig.3

3 BEAM SPECIMENS AND BENDING TESTS

3.1 *Beam specimens , bending tests and crack-repairing*

Beam specimens were made with the dimension of 40 mm x 40 mm x 160 mm (BxHxL). In this study, beams were also made that were reinforced by a steel bar with a diameter of 2.0 mm as compressive reinforcement at the top of the beam. Figure 4 shows dimensinos of a beam specimens with and without top steel reinforcement. Three-point bending tests were conducted to trigger cracking in beam specimens and to measure the force-deflection curves of the beams. The distance between supports was 100 mm and force was applied at the center of each beam using an actuator. Deflection of beams were measured by a linear voltage displacement transducer (LVDT) installed at the center-bottom of a beam. The set-up for the test is shown in Figure 5. After cracking, the widths of cracks were measured by a magnifying lens which was assembled to a smart-phone camera.

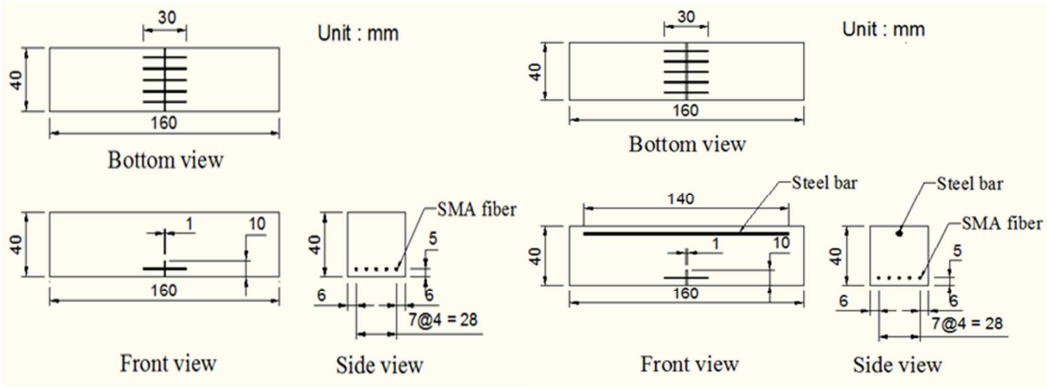

(a) Without top steel reinforcement (b) with top steel reinforcement

Figure 4 Dimension of a beam specimen

After the shape of a crack was captured, its width was calculated using an application-program in the smart-phone. Then, a cracked beam was repaired following the below procedure:

(1) injecting epoxy into a crack using a syringe; for this , the epoxy should have high fluidity.
(2) heating the SMA fibers inside a crack to activate the shape memory effect and induce recovery stress to close the crack.
(3) the epoxy inside the crack is compressed and sticks both cracked surfaces together.

Because of the high fluidity of the epoxy, it takes a relatively long time for the epoxy to cure. After a day, the widths of the closed cracks were measured again, and crack-repaired beams were tested again to confirm the recovery of flexural strength. The type of epoxy and hardener was EPOKIKDO YD-114 and DOCURE KH-816 respectively. They were mixed at the rate of 1:1 in weight. The curing condition of epoxy is 24 hours at room temperature and 2hours at 80 ℃

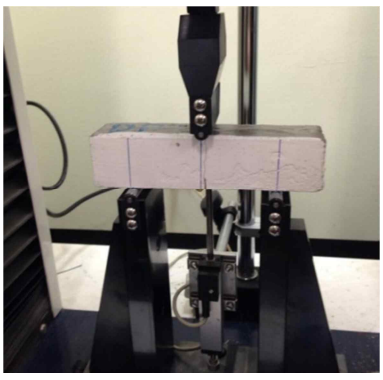

Figure 5 Test set-up for a three-point bending test

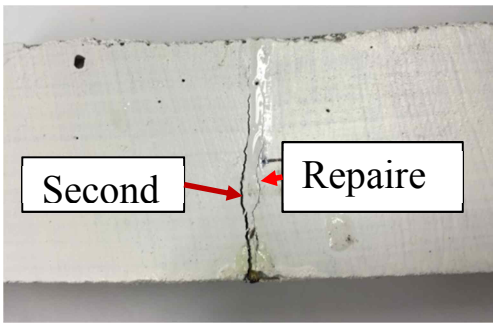

Figure 6 Cracking at a deviated location from the repaired crack

4 EXPERIMENTAL RESULTS AND DISCUSSIONS

4.1 Force-deflection curves

A pre-strained martensitic SMA under a deformation constraint generates recovery stress upon heating to above the A_f temperature. The remaining stress after cooling at room temperature is called residual stress. For the NiTiNb fiber, the average peak forces were 1.42 and 1.43 kN, respectively. Regardless of whether or not there was top steel reinforcement, the average peak forces of the reference beams did not vary much. Figure 7 shows a part of the force-deflection curves. It compares the force-deflection curves of beams reinforced by SMA fibers with those of the as-built beams. In this study, successful repair means that the second peak force significantly exceeds the residual force of the first test. Repaired peak strength was larger than original peak strength in graphs. In general, when the repair of cracks was successful, the peak forces of the repaired beams were greater than those of the as-built beams. Also, the loading paths of the repaired beams followed those of the as-built beams, thus, the flexural stiffnesses of the as-built and repaired beams were similar. When the repaired peak force was much greater than that of the as-built, a second crack developed at a deviated location from the first crack; because of this, relatively large flexural strength and elastic deflection were observed in the successful repair cases. Figure 6 shows such a case of cracking at a deviated location from the initial crack.

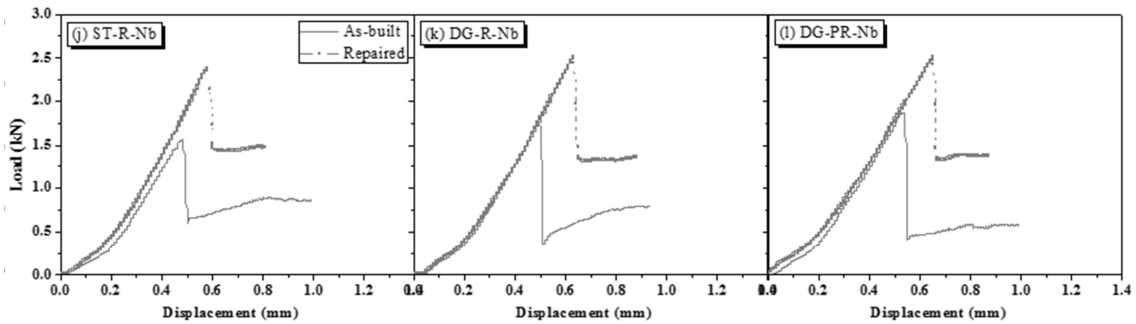

Figure 7. Force-deflection curves of beams with SAM fiber (only for three cases among twelve cases)

4.2 Peak force and recovery ratio of flexural strength

The average peak forces at the flexural strength of the as-built and repaired beams are shown in Table 1, including their standard deviations. All specimens with SMA fibers showed increment of flexural strength compared with those of the plain beams. The average peak forces for the beams with NiTi and NiTiNb fibers were 1.70 and 1.73 kN, respectively. The flexural strength recovery (FSR) ratio was calculated to estimate the incremental ratio of flexural strength due to using SMA fibers following the equation, and the results are listed in the 7th column of Table 1:

$$FSR = \frac{P_{re} - P_{as}}{P_{as}} \tag{1}$$

Table 1. Average peak forces

SMA	Fiber	As-built (kN)		Repaired (kN)		Flexural Strength Recovery ratio (%)
		μ	σ	μ	σ	
NiTi	ST	1.61	0.01	2.25	0.02	39.8
	DG	1.85	0	0.59	0	-68.1
	DG-P	1.64	0.08	1.01	0.14	-38.4
	ST-R	1.79	0.092	2.00	0.408	11.7
	DG-R	1.74	0.148	1.89	0.559	8.6
	DG-PR	1.59	0.045	1.81	0.665	13.8
NiTiNb	ST-Nb	1.92	0.096	3.18	0.390	65.6
	DG-Nb	1.74	0.164	3.05	0.540	75.3
	DG-P_Nb	1.62	0.057	1.34	0.258	-17.3
	ST-R-Nb	1.70	0.107	2.36	0.178	38.8
	DG-R-Nb	1.74	0.132	2.60	0.333	49.4
	DG-PR-Nb	1.67	0.116	1.58	0.440	-5.4

where P_{re} and P_{as} represent the peak force values of the repaired and as-built beams. When an FSR ratio is positive, the peak force of the repaired beam is greater than that of the corresponding as-built beam. The result indicates that the NiTiNb fibers have more capacity to recovery the flexural strength of cracked beams than the NiTi fibers. It appears that this result was caused by the difference in the residual stresses of the two SMA fibers. The NiTiNb fiber can provide more resistance to crack-opening than the NiTi fiber. In addition, the residual stress of the fibers was still present after crack-opening during a bending test of a repaired beam. After unloading, it can close the crack. Based on this point, the NiTiNb fiber is superior to the NiTi fiber. Between the ST and DG fibers, they did not have a significant effect on the FSR ratio, regardless of the type of alloy.

4.3 Crack-recovery ratio versus flexural strength recovery ratio

Crack-widths were measured using the magnifying lens before and after crack-repairing. The average values of the widths are listed in Table 2, and Crack-recovery ratio (CRR) was calculated using the following equation:

$$CRR = \frac{\Delta w}{w_o} \tag{2}$$

where w_o is the crack-width before repair, and Δw is the recovered width of a crack. A comparison of the NiTi and NiTiNb alloys shows that the CRRs of the two alloys' fibers would be similar since they showed similar maximum closing stresses due to recovery stress. However, when an external load was applied, the residual stress at ambient temperature would be critical to preserve crack-closing capacity. It appears that the paper inside a crack may absorb the epoxy injected and disturbed the bond between cracked surfaces. In this study, they did not make a difference in flexural strength recovery ratio in comparison with ST fibers. Therefore, it can be concluded that the crack-closing capacity of SMA fibers is not a critical factor in the flexural strength recovery of a cracked beam. Meanwhile, the NiTiNb SMA fibers showed larger flexural strength recovery ratios than the NiTi SMA fibers. The result between DG and DG-Nb fiber indicates that small closing stress of the SMA fibers is sufficient to close a crack and to bond cracked surfaces using epoxy application. For the repair of cracks, uniform

distribution of adhesive on cracked surfaces is critical; therefore, an efficient method for applying epoxy into cracks should be studied for the practical use of SMA fibers.

Table 2. Crack- widths and crack recovery ratios of specimens

SMA	Fiber	Initial crack width w_i (mm)	Repaired crack width w_r (mm)	Recovery of crack width $\Delta w = w_i - w_r$ (mm)	Crack-closing recovery ratio $\frac{\Delta w}{w_i} \times 100$ (%)
NiTi	ST	0.53	0.36	0.16	32.1
	DG	0.47	0.38	0.09	19.1
	DG-P	0.62	0.13	0.49	79.0
	ST-R	0.52	0.20	0.32	61.5
	DG-R	0.4	0.12	0.28	70.0
	DG-PR	0.41	0.09	0.32	78.0
NiTiNb	ST-Nb	0.52	0.30	0.22	42.3
	DG-Nb	0.34	0.32	0.02	5.9
	DG-P-Nb	0.48	0.36	0.12	25.0
	ST-R-Nb	0.36	0.19	0.17	47.2
	DG-R-Nb	0.39	0.18	0.21	53.8
	DG-PR-Nb	0.34	0.08	0.26	76.5

5 CONCLUSIONS

In this study, crack-repairing tests were performed on mortar beams fabricated using two types of SMA fibers, namely, NiTi and NiTiNb. They were manufactured by cold-drawing to introduce prestrain, and they showed similar recovery stress at high temperature but totally different residual stresses at ambient temperature. Because of the wide temperature hysteresis of the NiTiNb SMA, the NiTiNb SMA fibers showed approximately 8.0 times greater residual stress than the NiTi SMA fibers. In the tests, there were three types of fibers for each alloy, namely, straight, dog-bone, and dog-bone with paper-wrapping. Half of the specimens of each type had a steel reinforcement at the top of beams. Epoxy was applied between crack surfaces to bond the cracks, and then the SMA fibers were activated using a hot gun to induce recovery stress. Twice bending tests for each beam were conducted before and after the cracks were repaired. The top steel reinforcement appeared not to effect the flexural strength recovery ratios of the repaired beams since its main role was to prohibit crack-propagation to the top of the beams. When epoxy was adequately injected between cracked surfaces, a second crack developed at a deviated location from the initial crack. This indicates that the tensile strength of repaired cracks is greater than that of mortar. The straight and dog-bone fibers showed similar crack-repairing capacities; their flexural strengths exceeded the corresponding initial flexural strengths achieved by repairing except for the NiTi dog-bone fiber. However, the dog-bone fibers with paper-wrapping showed less flexural strength after repair. Most of them did not recover the initial flexural strength even though they showed greater crack-closing capacity; only the DG-PR fiber fully recovered the flexural strength and showed a positive flexural strength recovery ratio. It

appears that the used paper absorbed the applied epoxy; thus, the adhesion between cracked surfaces became poor. This indicates that the adequate application of the epoxy is more important for repairing cracks than the crack-closing capacity. The NiTiNb fibers showed a larger flexural strength recovery ratio than the NiTi fibers because of the greater residual stress of the NiTiNb SMA at ambient temperature. The residual stress of the fiber after cooling functioned like prestress on the mortar; this is different from the closing stress of the fibers due to the recovery stress at high temperature. It can be said that the greater residual stress of the NiTiNb fibers provided more resistance to crack-initiation comparing with the NiTi fibers. This result corresponds to that of a previous study, which mentioned that SMA fibers inside mortar beams were heated before cracking and showed relatively high resistance to cracking since the recovery or residual stress induced by heating provided prestress on the mortar. The results of this study indicate that the adhesion of epoxy and the residual stress of SMA fibers are critical for the perfect repair of cracks in mortar beams. However, the crack-closing capacity of the fibers was less significant than the above two factors. The injection of the epoxy used in this study seems not to be a practical method. A more practical and effective method should be found since the adhesion of cracks is critical for repairing cracks.

Acknowledgement

This study was supported by the Basic Science Research Program through the National Research Foundation of Korea funded by the Ministry of Education, Science and Technology (Project No. NRF 2012-R1A2A2A06-045603; 2013-R1A12-058208).

References

Choi E, Kim D, Chung Y S, and Nam T, 2014, Bond-slip characteristics of SMA reinforcing fibers obtained by pull-out tests, *Materials Research Bulletin,* 58 28-31.

Choi E, Hu J W, Lee J H and Cho B S, 2015, Recovery stress of shape memory alloy wires induced by hydration heat of concrete in reinforced concrete beams J. Intelligent, *Materials Systems and Structures*, 26(1): 29-37.

Deng Z, Li Q and Sun H, 2006, Behavior of concrete beam with embedded shape memory alloy wires, *Engineering Structures*, 28:1691-1697.

Kim DJ, Kim HA, Chung YS and Choi E, 2014, Pullout resistance of straight NiTi shape memory alloy fibers in cement mortar after cold drawing and hear treatment, *Composite: Part B*, 67: 588-594.

Li H, Liu Z and Ou J, 2006, Behavior of a simple concrete beam driven by shape memory alloy wires, *Smart Materials and Structures*, 15 1039-1046.

Li L, Li Q and Zhang F ,2007, Behavior of Smart Concrete Beams with embedded shape memory alloy bundles, *J. Intelligent Material Systems and Structures*, 18: 1003-1014.

Li H, Liu Z and Ou J, 2008, Experimental study of a simple reinforced concrete beam temporarily strengthened by SMA wires followed by permanent strengthening with CFRP plates, *Engineering Structures*, 30, 716-723.